Plant Growth Regul (2017) 83:27–41
DOI 10.1007/s10725-017-0281-4

ORIGINAL PAPER

Regulation of ZnO nanoparticles-induced physiological and molecular changes by seed priming with humic acid in *Oryza sativa* seedlings

Mohamed S. Sheteiwy[1,2] · Qian Dong[1] · Jianyu An[1] · Wenjian Song[1] · Yajing Guan[1] · Fei He[1] · Yutao Huang[1] · Jin Hu[1]

Received: 21 March 2017 / Accepted: 14 May 2017 / Published online: 27 May 2017

Abstract The present investigation explored the capability of priming treatment with 250 mg L^{-1} of humic acid (HA) to improve nano-ZnO tolerance of two rice cultivars seedlings (Zhu Liang You 06 and Qian You No. 1). The results showed that seed germination, seedling growth, total soluble protein, sugar and starch contents significantly improved by seed priming with HA especially under high nano-ZnO stress (500 and 750 mg L^{-1}) as compared to unprimed seeds. In contrast, electrolyte leakage significantly increased after exposure to 500 and 750 mg L^{-1} nano-ZnO, but decreased obviously after HA priming in both cultivars. Abscisic acid (ABA) content in the seeds germinated under nano-ZnO stress was higher than those grown under non-stress condition; while gibberellins (GA) content decreased under nano-ZnO stress. HA priming down-regulated the relative expression levels of *OsABA8ox2* and *OsNCED1*, which were key genes in ABA biosynthesis and catabolism of rice seeds. In contrast, up-regulation in *OsGA20ox2* and *OsGA3ox1* were induced by HA priming. The histochemical analysis reported that higher concentration of hydrogen peroxide (H_2O_2) and superoxide radical ($O_2\cdot-$) were observed in stressed roots with nano-ZnO as compared with non-stress condition, indicating reduction of root cell viability and severe oxidative burst. However, HA priming reduced obviously H_2O_2, $O_2\cdot-$, antioxidant enzymes activities (SOD, POD, CAT) and malondialdehyde (MDA) content of rice seedlings under stress. Significant increases in dehydroascorbate reductase (DHAR) and monodehydroascorbate reductase (MDAR) activities were observed in nano-ZnO stressed seedlings, but they were diminished evidently by HA priming. In addition, the improvement of HA on cell ultra structure of root tip and leaf mesophyll was detected under nano-ZnO stress especially 750 mg L^{-1} concentration. Therefore, it was suggested that HA priming could definitely improve the rice seed germination and seedling growth under nano-ZnO stress to some extent.

Keywords Seed priming · Antioxidant enzymes · *Oryza sativa* · Oxidative stress · Nano-ZnO · Gene expression

Introduction

Heavy metals-polluted soils are a major problem in arable land which can reduce crop yield and quality. The pollution with heavy metals can naturally occur through the erosion of certain rocks and minerals, but predominantly come from industrial use of chemical fertilizers, sewage, and agrochemicals industries. As previously stated, unlike most organic contaminants, heavy metals were non-biodegradable and could accumulate in living tissues, posing a great effect to human health and the environment ecosystem (Lesmana et al. 2009). The analysis of heavy metals in the land and agricultural water management in Africa has carried out for half of century (Valipour 2015), which have provided a list of strengths and weaknesses of the availability of the water and soils to be used for economic cultivation. Recently, it has reported that the concentrations of metal in soil about 1–1,00,000 ppm might be due to anthropogenic activities or the geological interactions of the soil

✉ Yajing Guan
vcguan@zju.edu.cn

[1] Seed Science Center, College of Agriculture and Biotechnology, Zhejiang University, Hangzhou 310058, China

[2] Department of Agronomy, Faculty of Agriculture, Mansoura University, Mansoura 35516, Egypt

profile (Blaylock and Huang 2000). Drainage played an important role to reduce heavy metals and improved soil quality (physical and chemical properties) in agriculture (Valipour 2013a, b; Viero and Valipour 2017).

The effect of nano-metals toxicity on plant growth and production is an interested area of research which has not been full clarified yet. Nano-ZnO have been naturally formed on the soil profile for millions of years and can be found almost everywhere in the environment. Additionally, nano-ZnO can be also formed through physical and chemical weathering of rocks and mineral near the surface of earth. These processes cause the unstable minerals under surface to dissolve or react with other phases (Kool et al. 2011). The utilization, synthesis and transfer of nanoparticles (NPs) will definitely accelerate their release to the environment. Furthermore, NPs formed as byproducts during many industrial processes. However, in the field of agriculture, the use of nanomaterials is relatively new exploration and the information about the NPs effect on water and soil still remain limited. Among many types of nanomaterials, zinc-based NPs are increasingly utilized for their conspicuous plasmonic and antibacterial properties (Pokhrel and Dubey 2013). Nano-ZnO are the most common Zn NPs which are being used as UV protection e.g. in personal care products, coating and paints, biosensors, electronic, and rubber manufacturing (Kool et al. 2011).

Under different environmental stresses, ROS e.g. H_2O_2 and $O_2{\cdot}-$, can be produced in stressed plant tissues (Zhu 2000). However, the activation of ascorbate peroxidase (APX), catalase (CAT), superoxide dismutase (SOD), peroxidase (POD) and glutathione reductase (GR) are considered to be the mechanisms underlying ROS detoxification in plants (Meloni et al. 2003). Moreover, several isomeric forms of SOD in plants have the potential to catalyze conversion of O_2^{-} to H_2O_2. Thereafter, CAT catalyzed the conversion of H_2O_2 into water in peroxisomes (Mahmoud et al. 2016).

Seed priming with HA has been usually used to decrease the time between seed sowing and seedling development as well as can also protects plants in water deficient-soils (Parera and Cantliffe 1994). Great progress has been made to understand the mechanisms underlying the mode of action of humic acid-induced defense of plants against oxidative stress. It has reported that HA at 300 and 450 ppm concentrations increased SOD, CAT and glutathione peroxidase enzyme activity (Moghadam 2013). Recently, it has been proposed that HA can precipitates in roots to decrease the transpiration rate and the water use efficiency of the roots under stress condition (Asli and Neumann 2010). It has been reported that ABA and GA have different pathways to control seed germination (Finch-Savage 2006). Up-regulation of ABA biosynthesis in *Arabidopsis thaliana* is proposed as one of the conceivable mechanisms that could intervene the glucose-incited delay in seed germination. Since the endogenous ABA level is regulated by the compatibility between ABA catabolism and ABA biosynthesis (Zhu et al. 2009). Moreover, improved of seed germination by GA is decreased by a low concentration of ABA (Liu et al. 2010).

To better understand the mechanisms and benefits effects of priming with HA for rice (*Oryza sativa*, L.) seedlings under nano-ZnO stress, several physiological and molecular parameters could be investigated in this study. Namely, germination percentage, seedling growth parameters, ABA and GA hormones activities were monitored to understand the physiological mechanism of plant under stress. To date, most of the previous studies have focused on the effect of seed priming through the physiological and morphological approaches. The present study focused on the morphological, physiological and molecular mechanism of HA priming on rice seedling under nano-ZnO stress. To give more precise evaluation of the beneficial effect of HA priming to increase rice seed germination under nano-ZnO stress, the relative transcript abundance of ABA and GA were studied at molecular levels after exposure to different nano-ZnO concentrations. The enzymes related to oxidative stress such as SOD, POD, CAT, APX, GR, GSH, DHAR and MDAR activities were also studied to disclose the oxidative defense of rice plants under nano-ZnO stress. Furthermore, the changes in the ultrastructure of leaf and root cells were studied using transmission electron microscopy analysis (TEM). The detection of ROS such as H_2O_2 and $O_2{\cdot}-$ in the roots were investigated using histochemical staining analysis.

Materials and methods

Plant material and seed germination

Two cultivars of rice cv. Zhu Liang You 06 (ZY) and Qian You No.1 (QY) were obtained from the Seed Science Center of Zhejiang University, China. Seeds were primed using the same method of Sheteiwy et al. (2016). Primed seeds were dried up to their original moisture content and the unprimed seeds were used as control (Ck, dry seed). HA were purchased from the International Humic Substances Society company. The concentrations of HA used for priming treatment were initially selected based on pre-experiment. In this preliminary experiment, different concentrations (0, 100, 250, 300 and 350 mg L^{-1}) of HA were investigated. Results showed that HA with 250 mg L^{-1} concentration significantly improved the germination percentage and seedling growth as compared to the others different concentrations of HA. For this reason, only 250 mg L^{-1} of HA was used in this study.

After priming treatment, seed germination tests were carried out and seed were exposed to different concentrations of nano-ZnO stress. For seed germination percentage and seedling growth parameters measurements, seedlings were harvested and the germination percentage was recorded after 14 days of treatments. Shoots and roots length of randomly selected ten seedlings and their dry and fresh weight were measured according to the method of Hu et al. (2016). Seedling vigor index was measured according to the method described by Sheteiwy et al. (2015).

Determination of ABA and GA contents

The ABA levels of rice was determined in the seeds with or without HA priming and stressed with 0, 250, 500 and 750 mg L^{-1} for 1 week using the method of Zhu et al. (2015). In brief, 0.2 g of the seeds treated for 7 days was separated from seedling and homogenized in 1 mL of distilled water and then vortexed overnight at 4 °C. Thereafter, the homogenates were centrifuged at 12,000×*g* for 10 min at 4 °C, after which the supernatant was used for determination of ABA using the radioimmunoassay (RIA) method as described by Zhu et al. (2015). seed sample (0.1 g) were frozen in liquid nitrogen for GA measurement and finely ground with 15 mL methanol containing 20% water (v/v) at 4 °C for 12 h. Endogenous GAs was determined as depicted by Zhu et al. (2015). For ABA and GA genes expression analysis, seed were separated from the seedlings and stored at −80 °C for their later respective analysis.

Biochemical analysis

Total soluble sugar and starch contents were determined in the shoots according to the method of Zhu et al. (2015). Soluble protein contents were measured according to the method portrayed by Bradford (1976). GR activity was determined according to the method of Schaedle and Bassham (1977). In brief, 200 mg of fresh shoot were homogenized by using mortar and pestle in 5 mL of 50 mM phosphate buffer (pH 7.6). The homogenate was centrifuged at 22,000×*g* at 4 °C for 30 min and the supernatant was used for enzymes determination. The specific activity of enzyme is expressed as μmol NADPH oxidized min^{-1} $(mg\ protein)^{-1}$. GSH activity was determined according to the method of Law et al. (1983).

In order to measure the antioxidant enzyme activities such as SOD, CAT, APX and POD, leaf samples (0.5 g) were taken per treatment and homogenized in 8 mL of 50 mM potassium phosphate buffer (pH 7.8) under ice cold conditions. Homogenate was centrifuged at 10,000×*g* for 20 min at 4 °C and the supernatant was used for the determination of the antioxidant enzymes according to the methods of Sheteiwy et al. (2017).

Determination of relative electrolyte leakage (REL)

For determination the electrolyte conductivity (dSm^{-1}) of seed leachate, 5 g of seeds were surface sterilized with $HgCl_2$ (1%) and washed in distilled water using four replications. Thereafter, seeds were soaked in 25 mL distilled water and incubated at 25 °C for 24 h. The leachate was transferred to another empty container and made the volume up to 25 mL by adding distilled water. The electrolyte leakage was measured in the seed leachate and expressed in dSm^{-1} (ISTA 2004).

Dehydroascorbate reductase (DHAR)

DHAR activity was determined using the method of Nakano and Asada (1981). The total reaction mixture consisted of 50 mM potassium phosphate buffer (pH 7.0), 2.5 mM GSH, 0.2 mM DHA and 0.1 mM EDTA in a final volume of 1 mL. The reaction was started by adding an aliquot of enzyme extract and increment of absorbance was recorded for 3 min with 30 s interval at 265 nm. Enzyme activity was expressed as μmol min^{-1} mg^{-1} protein of ascorbate formed.

Monodehydroascorbate reductase (MDAR)

MDAR activity was assayed by the method of Miyake and Asada (1992). MDAR was extracted by ascorbate oxidase using a reaction mixture (1 mL) containing 50 mM HEPES-KOH buffer, pH 7.6, 0.1 mM NADPH, 2.5 mM ascorbate, ascorbate oxidase (0.14U) and an aliquot of enzyme extract. MDAR activity was expressed as μmol min^{-1} mg^{-1} protein of NADPH oxidized.

Analysis of lipid peroxidation and reactive oxygen species (ROS)

Lipid peroxidation was measured as far as MDA content which was analyzed using the method of Zhou and Leul (1999). Superoxide radical ($O_2\cdot-$) was measured following the method of Jiang and Zhang (2003) with slight changes. Root sample (0.5 g) was homogenized in 3 mL of 65 mM potassium phosphate buffer (pH 7.8). The homogenate was then centrifuged at 5000 × g at 4 °C for 10 min. Thereafter, 1 mL of the supernatant was incubated at 25 °C for 24 h after mixed with 0.9 mL of 65 mM potassium phosphate buffer (pH 7.8) and 0.1 mL of 10 mM hydroxylamine hydrochloride. Thereafter, 1 mL of the mixture solution was incubated with 1 mL of 17 mM sulphanilamide and 1 mL of 7 mM a-naphthylamine at 25 °C for 20 min. The $O_2\cdot-$ rate in the supernatant was read by using spectrophotometer at 530 nm. For determination of H_2O_2 contents, 0.5 g of root was homogenized with 5.0 mL of 0.1%

trichloroacetic acid (TCA) using ice bath, then homogenate was centrifuged for 15 min at 12,000×*g* (Velikova et al. 2000). Then, 0.5 mL supernatant was mixed with 0.5 mL of 10 mM potassium phosphate buffer (pH 7.0) and 1 mL of 1 M KI was added. The H_2O_2 content in the supernatant was read by using spectrophotometer at 390 nm.

Expression analysis of ABA and GA pathway

Seven days-treated seeds, total RNA was isolated by using RNA isolation (Takara, Japan). 100 mg of frozen seed sample was ground in liquid nitrogen using a mortar and pestle. The RNA concentration was measured by NanoDrop 2000/2000c (Thermo Scientific, USA). Quantitative real-time PCR (QRT-PCR) was carried out using three biological replications for each treatment and three technical replications were used for each biological replicate. Primers used in QRT-PCR are shown in Table 1, and *ACT1* was used as a control to measure the transcript levels of the other studied genes. The PCR program used in this study was the same as described by Sheteiwy et al. (2015).

Ultrastructure and histochemical staining studies

The ultrastructural changes of leaf and root samples were detected according to the method of Sheteiwy et al. (2015). Samples were then processed for EDS analysis (Zn microlocalization studies) using manufacturers standard protocols (EDAX GENESIS XM2 30TEM) according to the method of Daud et al. (2015). H_2O_2 and $O_2\cdot-$ contents of roots was physically detected by DAB and NBT staining, respectively. The stained roots were photographed using microscope equipped with camera provided with high digital resolution (Leica MZ- g5, Germany).

Statistical analysis

Completely randomized design in factorial experiment was used in this study. The results are mean of three replicates ± standard deviation (SD). The data were arcsin-transformed before analysis according to $\hat{y} = \arcsin$ [sqr (×100)]. SPSS v16.0 software (SPSS, Inc., Chicago, IL, USA) was used for analyzing the data. Analysis of variance (ANOVA) was carried out, followed by Duncan's multiple range tests at the $p < 0.05$ and *0.01* levels.

Results

Seed germination and plant growth

In the present study, nano-ZnO stress treatment decreased seed germination percentage, shoot and root length, seedling dry and fresh weight and seedling vigor index; however, HA priming could definitely improve seedling growth of both studied cultivars under nano-ZnO stress as compared with the unprimed control (Table 2). As compared with the control (92.66%), germination percentage was significantly reduced in ZY at 500 mg L^{-1} (84.00%) and 750 mg L^{-1} (62.66%) (Table 2). For QY, its seed germination was higher than ZY and significant decreases in seed germination were only observed under 750 mg L^{-1} of nano-ZnO stress. HA priming increased obviously germination percentage of both rice cultivars, especially QY under 750 mg L^{-1} of nano-ZnO stress (Table 2). As compared with control plants, except unprimed seeds in lower nano-ZnO stress, root and shoot length significantly reduced in stressed seedlings of both cultivars under all nano-ZnO concentrations (Table 2). In addition, significant decreases in seedling dry weight and fresh weight were observed in two cultivars at 750 mg L^{-1} of nano-ZnO concentration (Table 2). While seedling vigor index of both cultivars were significantly decreased under nano-ZnO stress. In which, QY recorded higher seedling vigor index as compared with ZY (Table 2). HA priming could improve seedling vigor index of QY under 750 mg L^{-1} nano-ZnO stress, which was significantly higher than ZY.

Table 1 Sequences of oligonucleotide primers used in QRT-PCR

Locus	Primer name	Primer orientation	Sequence (5′–3′)
OsNCED1	AY838897-F	Forward	CTCACCATGAAGTCCATGAGGCTT
	AY838897-R	Reverse	GTTCTCGTAGTCTTGGTCTTGGCT
OsABA8ox2	AK120757-F	Forward	CAGACGAGGAGCATGACACTCA
	AK120757-R	Reverse	GTTCCTGAACAGAGGCATCACC
OsGA3ox1	AB056519-F	Forward	CGGACTCGGGCTTCTTCACCT
	AB056519-R	Reverse	CGAGGAAGTAGCCGAGCGAGAC
OsGA20ox2	AB077025-F	Forward	CGCCGACTACTTCTCCAGCACC
	AB077025-R	Reverse	GCTGTCCGCGAAGAACTCCCT
ACTIN	AY212324-F	Forward	GGTATTGTTAGCAACTGGGATG
	AY212324-R	Reverse	GATGAAAGAGGGCTGGAAGA

Table 2 Effects of seed priming with HA (250 mg L^{-1}) on germination percentage (GP, %), root length (cm), shoot length (cm), seedling dry weight (SDW, g/10 seedlings), seedling fresh weight (SFW, g/10 seedlings) and seedling vigor index (SVI) of two cultivars of *Oryza sativa* under different concentrations of nano-ZnO stress (mg L^{-1})

Cultivars	HA priming	Nano-ZnO	GP	Root length	Shoot length	SFW	SDW	SVI
ZY	0	0	92.66 ± 1.1c–e	9.00 ± 0.2bc	8.10 ± 0.2cd	0.087 ± 0.001a–c	0.0410 ± 0.001b–e	1585 ± 34.40d–f
		250	90.66 ± 2.3ef	8.50 ± 0.2d	7.59 ± 0.2d	0.085 ± 0.001bc	0.0393 ± 0.003d–f	1482 ± 35.84fg
		500	84.00 ± 2.0g	7.56 ± 0.2e	6.50 ± 0.2e	0.082 ± 0.002cd	0.0370 ± 0.001g	1234 ± 58.32h
		750	62.66 ± 3.0j	6.16 ± 0.1f	5.10 ± 0.1f	0.074 ± 0.003e	0.0310 ± 0.001i	710 ± 42.82j
	250	0	98.00 ± 0.05ab	10.63 ± 0.1a	9.40 ± 0.1a	0.088 ± 0.009bc	0.0430 ± 0.001ab	1927 ± 65.25b
		250	94.66 ± 1.1bc	9.06 ± 0.2b	8.16 ± 0.2cd	0.088 ± 0.002a-c	0.0413 ± 0.005b–d	1622 ± 36.38de
		500	89.33 ± 1.1f	8.50 ± 0.1d	7.40 ± 0.1d	0.083 ± 0.004b-d	0.0390 ± 0.001e–g	1429 ± 29.53g
		750	77.33 ± 1.1h	7.43 ± 0.1e	6.33 ± 0.1e	0.077 ± 0.003de	0.0327 ± 0.005hi	1072 ± 27.42i
QY	0	0	96.00 ± 2.0bc	9.20 ± 0.2b	8.10 ± 0.2c	0.088 ± 0.001a-c	0.0423 ± 0.002a–c	1693 ± 63.51cd
		250	93.33 ± 1.1cd	8.70 ± 0.2cd	7.65 ± 0.2cd	0.086 ± 0.001bc	0.0403 ± 0.005c–e	1541 ± 32.90e–g
		500	89.33 ± 3.0f	7.76 ± 0.2e	6.67 ± 0.2e	0.083 ± bc0.002d	0.0377 ± 0.001fg	1308 ± 74.33h
		750	66.66 ± 4.1i	6.36 ± 0.1f	5.31 ± 0.1f	0.075 ± 0.003e	0.0320 ± 0.001hi	781 ± 34.48j
	250	0	100.00 ± 0.3a	10.83 ± 0.1a	9.77 ± 0.1a	0.093 ± 0.003a	0.0440 ± 0.001a	2070 ± 10.0a
		250	97.00 ± 1.1b	9.26 ± 0.2b	8.86 ± 1.0b	0.089 ± 0.002bc	0.0423 ± 0.005a–c	1765 ± 130.42c
		500	95.00 ± 2.3bc	8.70 ± 0.1cd	7.65 ± 0.1cd	0.087 ± 0.002a–c	0.0400 ± 0.001de	1563 ± 32.60ef
		750	82.00 ± 3.0g	7.63 ± 0.1e	6.60 ± 0.1e	0.078 ± 0.003de	0.0337 ± 0.005h	1250 ± 169.43h

The same letters within a column indicate there was no significant difference at a 95% probability level at the $p \leq 0.05$ level

HA humic acid, nano-ZnO zinc oxide nanoparticles

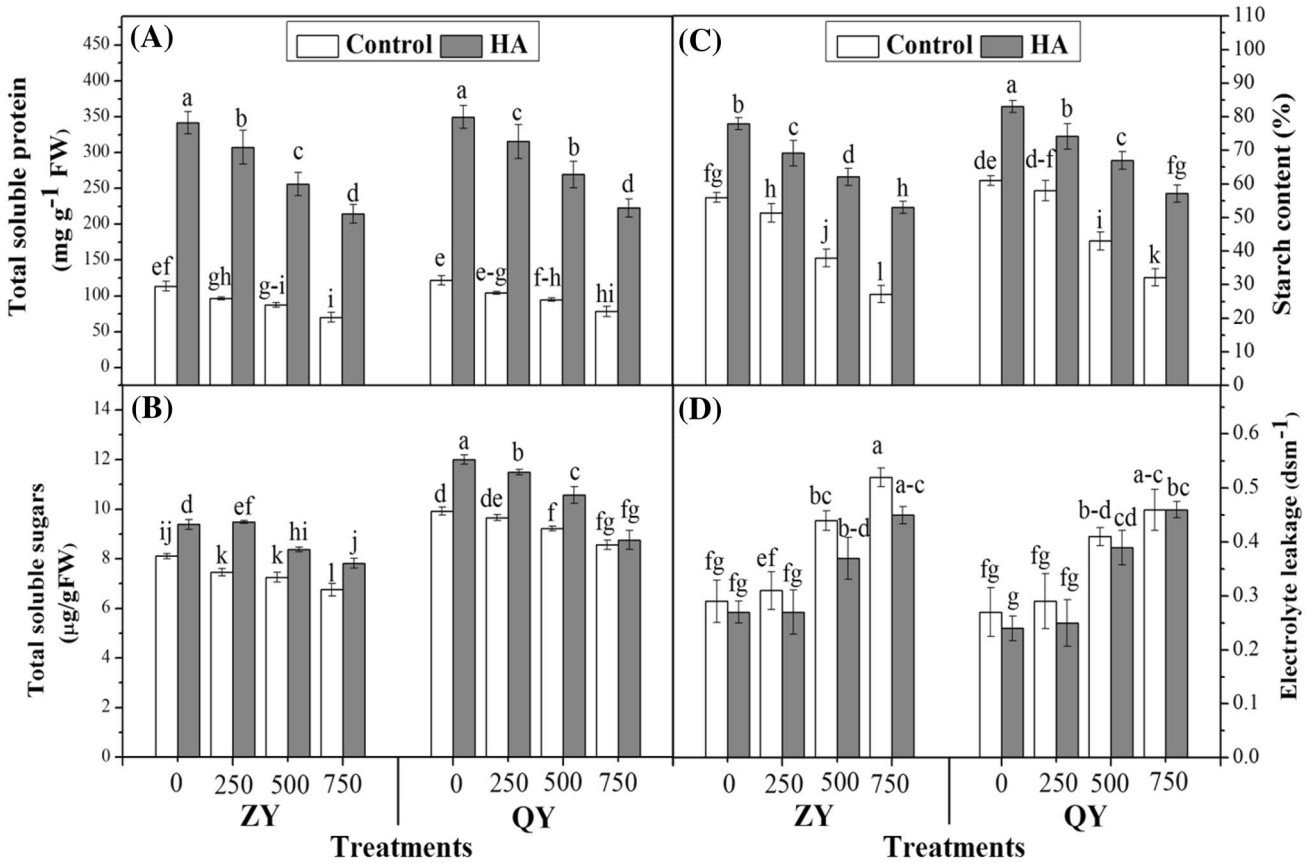

Fig. 1 Effects of seed priming with HA (250 mg L^{-1}) on **a** total soluble protein, **b** total soluble sugar, **c** starch content and **d** electrolyte leakage of two cultivars of *Oryza sativa* under different concentrations of nano-ZnO stress. Values were the means ± SD of three replications. Variants possessing the same letter were not statistically significant at $p \leq 0.05$

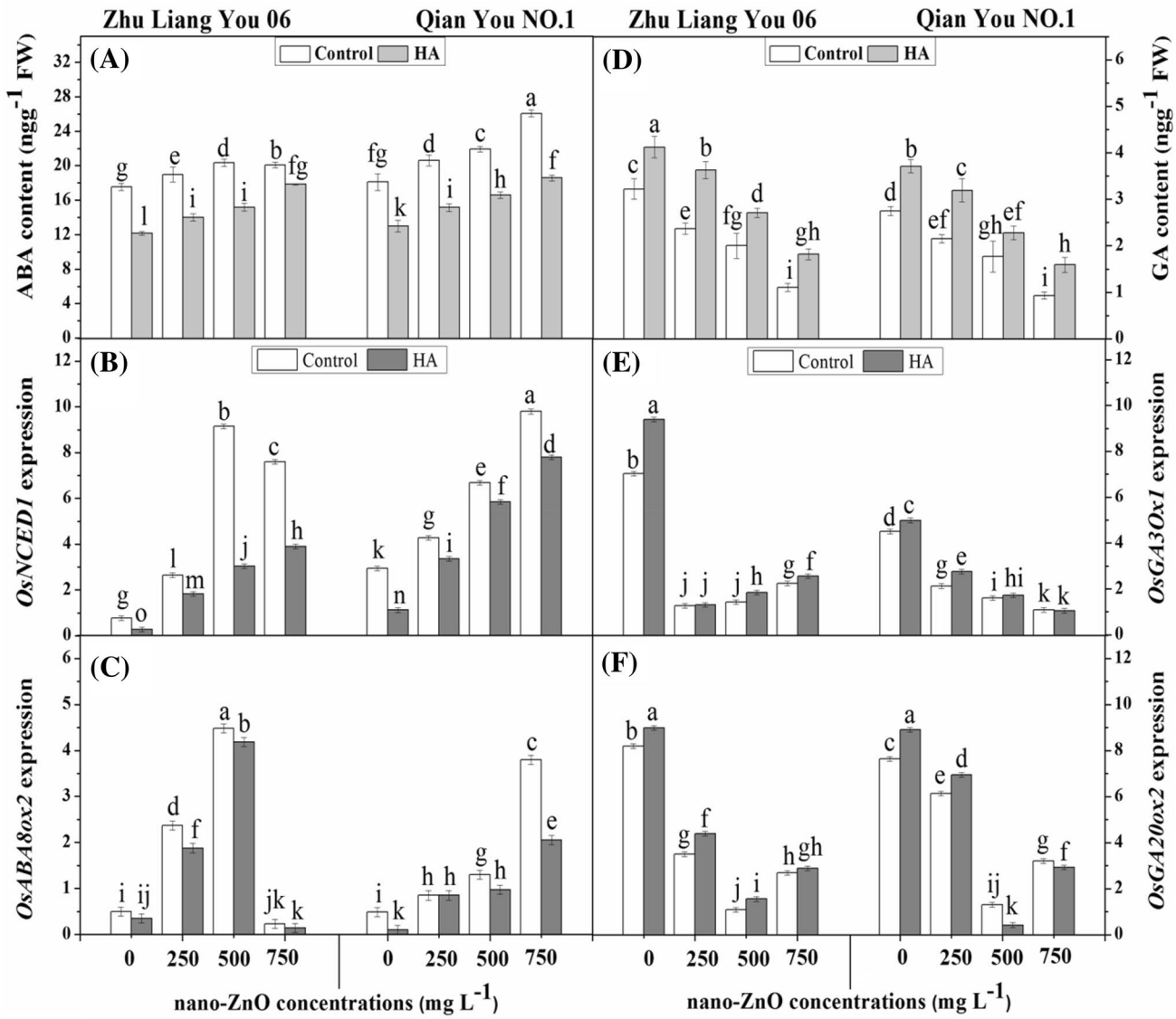

Fig. 2 Effects of seed priming with HA (250 mg L^{-1}) on **a** ABA content, **b** transcript abundance of *OsNCED1*, **c** transcript abundance of *OsABA8ox2*, **d** GA content, **e** transcript abundance of *OsGA3ox1*, **f** transcript abundance of *OsGA20ox2* in the shoots of two cultivars of *Oryza sativa* under different concentrations of nano-ZnO stress. Values were the means ± SD of three replications. Variants possessing the same letter were not statistically significant at $p \leq 0.05$

The contents of total soluble protein, sugar, starch and electrolyte leakage

Nano-ZnO stress induced gradual decrease of total soluble protein in both studied cultivars as compared with the control. HA priming improved the total soluble protein in both cultivars under stress, and the highest values were observed in primed seeds of QY under non-stress condition (Fig. 1a). Total soluble sugars were recorded higher in QY than in ZY under each nano-ZnO concentration, and its highest values were recorded with primed seeds of QY under 0 mg L^{-1} nano-ZnO concentration. HA priming could significantly increase total soluble sugars in both cultivars (Fig. 1b). Significant decreases in starch content were recorded in both cultivars under all nano-ZnO concentrations, and degree of reduction was associated with increases in nano-ZnO concentrations (Fig. 1c). Based on the relevant results, electrolyte leakage was significantly increased in both cultivars after exposure to 500 and 750 mg L^{-1} concentrations of nano-ZnO. However, seed priming with HA resulted in a decrease of the electrolyte leakage in both cultivars under stress as compared to the unprimed seeds (Fig. 1d).

Table 3 Correlation analysis between molecular and biochemical parameters with seed germination and seedling characters primed with HA and exposed to nano-ZnO stress

Parameters	GP	SVI	Root length	Shoot length
Total soluble protein	0.562*	0.654**	0.685**	0.693**
Total soluble sugar	0.698**	0.754**	0.726**	0.749**
Starch content	0.852**	0.916**	0.922**	0.929**
Electrolyte leakage	−0.877**	−0.912**	−0.899**	−0.925**
ABA	−0.805**	−0.858**	−0.877**	−0.876**
GA	0.838**	0.910**	0.937**	0.941**
OsNCED1	−0.725**	−0.788**	−0.835**	−0.833**
OsABA8ox2	−0.262	−0.351	−0.387	−0.386
OsGA3ox1	0.423	0.561*	0.654**	0.615**
OsGA20ox2	0.506*	0.664**	0.716**	0.724**

*, **Indicate correlation significance at the *0.05* and *0.01* probability levels, respectively

GP germination percentage, *SVI* seedling vigor index, *ABA* abscisic acid, *GA* gibberellins

ABA and GA catabolism and their transcription levels

A significant increase of ABA level was observed with increasing nano-ZnO concentrations in both cultivars (Fig. 2a). Based on the results, seed priming with HA significantly reduced the level of ABA in both cultivars under different concentrations of nano-ZnO, and the ABA levels were found to be higher in the unprimed seeds of QY under stress condition (Fig. 2a). GA levels were significantly reduced with increasing nano-ZnO concentration in both cultivars as compared to the control (Fig. 2d). Seed priming with HA significantly enhanced the GA levels under different concentrations of nano-ZnO in both cultivars. Furthermore, the highest levels of GA were found in the primed seeds of ZY (Fig. 2d).

To understand the mechanism underlying the reduction of seed germination caused by nano-ZnO stress, the expressions of ABA and GA genes were analyzed through the molecular level (Fig. 2b, c, e, f). The relative expression of *OsNCED1* and *OsABA8ox2* were significantly down regulated in both cultivars without priming after exposure to all nano-ZnO concentrations. In ZY, up regulation of *OsNCED1* and *OsABA8ox2* were observed only at 500 mg L^{-1} concentration of nano-ZnO. Higher concentration of nano-ZnO (750 mg L^{-1}) resulted in down-regulation of *OsABA8ox2* gene expression level in ZY (Fig. 2c), despite the highest content of ABA in the stressed seedling with high concentration of nano-ZnO reflecting a feedback regulation of HA under stress (Fig. 2a). The expression level of *OsGA3ox1* decreased obviously in both cultivars, except for ZY exposed to 500 and 750 mg L^{-1} of nano-ZnO (Fig. 2e). Similarly, significant reduction in the expression of *OsGA20ox2* in both cultivars was observed under nano-ZnO stress, except 750 mg L^{-1} concentration (Fig. 2f). The

Table 4 Effects of seed priming with HA (250 mg L^{-1}) on SOD (U mg^{-1} protein), POD (μmol min^{-1} mg^{-1} protein), APX (μmol min^{-1} mg^{-1} protein), CAT (μmol min^{-1} mg^{-1} protein) activities and MDA contents (nmol mg^{-1} protein) in shoots of two cultivars of *Oryza sativa* under different concentrations of nano-ZnO stress (mg L^{-1})

Cultivars	HA priming	Nano-ZnO	SOD	POD	APX	CAT	MDA
ZY	0	0	685.71 ± 38.09e	2.50 ± 0.31fg	2.06 ± 0.10fgh	5.38 ± 0.09e	5.96 ± 0.45f
		250	787.30 ± 58.019d	3.17 ± 0.09cd	2.01 ± 0.015h	5.63 ± 0.57cd	8.25 ± 0.45cd
		500	901.59 ± 21.99c	3.49 ± 0.095c	1.97 ± 0.024h	5.82 ± 0.085c	9.32 ± 0.95b
		750	1130.2 ± 95.87a	4.89 ± 0.16a	1.92 ± 0.09h	6.32 ± 0.28a	12.08 ± 0.26a
	250	0	507.94 ± 21.99hi	2.08 ± 0.045hi	2.41 ± 0.09a	2.94 ± 0.045k	1.68 ± 0.26i
		250	546.03 ± 21.99ghi	2.20 ± 0.057ghi	2.34 ± 0.015ab	3.19 ± 0.057ij	4.58 ± 0.45gh
		500	584.13 ± 21.99gh	2.38 ± 0.04fgh	2.28 ± 0.09abc	3.42 ± 0.029h	5.81 ± 0.26 f
		750	698.41 ± 43.98e	2.62 ± 0.1f	2.20 ± 0.015cde	3.98 ± 0.33f	7.49 ± 0.26de
QY	0	0	609.52 ± 38.09fg	2.35 ± 0.32fgh	2.18 ± 0.015def	5.34 ± 0.085e	5.50 ± 0.45f
		250	673.02 ± 79.30ef	3.00 ± 0.09e	2.07 ± 0.015fgh	5.59 ± 0.057d	7.34 ± 0.45e
		500	825.40 ± 21.99d	3.34 ± 0.10cd	2.03 ± 0.024gh	5.79 ± 0.085cd	8.86 ± 0.95bc
		750	990.48 ± 38.09b	3.99 ± 0.54b	1.99 ± 0.09h	6.04 ± 0.012b	11.46 ± 0.45a
	250	0	431.75 ± 21.99j	1.92 ± 0.045i	2.29 ± 0.34abc	2.91 ± 0.045k	1.22 ± 0.26i
		250	469.84 ± 21.99ij	2.03 ± 0.11hi	2.40 ± 0.015a	3.15 ± 0.057j	4.12 ± 0.45h
		500	507.94 ± 21.99hij	2.21 ± 0.04ghi	2.35 ± 0.09ab	3.39 ± 0.029hi	5.35 ± 0.26g
		750	558.73 ± 21.99gh	2.28 ± 0.02fgh	2.26 ± 0.015abc	3.65 ± 0.069g	7.03 ± 0.26e

The same letters within a column indicate there was no significant difference at a 95% probability level at the $p \leq 0.05$ level

HA humic acid, nano-ZnO zinc oxide nanoparticles, *SOD* superoxide dismutase, *POD* peroxidase, *APX* ascorbate peroxidase, *CAT* catalase, *MDA* malonaldahyde

Table 5 Effects of seed priming with HA (250 mg L^{-1}) on H_2O_2 (nmol g^{-1} FW), $O_2\cdot-$ contents (nmol min^{-1} g^{-1} FW), GR (mmol min^{-1} mg^{-1} protein), GSH (mmol min^{-1} mg^{-1} protein), DHAR (μmol min^{-1} mg^{-1} protein) and MDAR (μmol min^{-1} mg^{-1} protein) activities in shoots of two cultivars of *Oryza sativa* under different concentrations of nano-ZnO stress (mg L^{-1})

Cultivars	HA priming	Nano-ZnO	H_2O_2	$O_2\cdot-$	GR	GSH	DHAR	MDAR
ZY	0	0	1.76 ± 0.34 c–e	3.52 ± 0.070b	9.54 ± 0.57hi	7.53 ± 0.37hi	0.250 ± 0.14g	0.0431 ± 0.003hi
		250	2.24 ± 1.29f–h	3.91 ± 0.067b	12.68 ± 0.78f	9.17 ± 0.79ef	0.297 ± 0.020de	0.0533 ± 0.004fg
		500	3.01 ± 0.026 ab	4.33 ± 0.107ab	15.31 ± 0.57d	11.17 ± 0.57c	0.357 ± 0.014c	0.0667 ± 0.003d
		750	3.36 ± 0.092 a	4.89 ± 0.290ab	17.07 ± 0.57c	12.55 ± 0.21b	0.447 ± 0.017a	0.0856 ± 0.003b
	250	0	1.58 ± 0.067g–i	2.44 ± 0.306b	5.90 ± 0.43j	5.90 ± 0.21j	0.104 ± 0.010k	0.0349 ± 0.003jk
		250	1.97 ± 0.106 e–g	10.68 ± 0.361a	9.16 ± 0.43i	6.90 ± 0.21i	0.164 ± 0.021j	0.0246 ± 0.004l
		500	2.68 ± 0.040 bc	2.93 ± 0.314b	11.17 ± 0.21g	8.78 ± 0.57fg	0.238 ± 0.014gh	0.0405 ± 0.003ij
		750	2.86 ± 0.120 a–c	3.84 ± 0.450b	12.42 ± 0.99f	10.67 ± 0.57cd	0.288 ± 0.032ef	0.0513 ± 0.006g
QY	0	0	1.47 ± 0.146g–h	5.06 ± 0.266ab	11.67 ± 0.37fg	9.52 ± 0.33e	0.214 ± 0.014hi	0.0508 ± 0.003g
		250	1.81 ± 0.096f–h	5.51 ± 0.307ab	15.44 ± 0.65d	10.42 ± 0.21d	0.261 ± 0.020fg	0.0610 ± 0.004de
		500	2.39 ± 0.055b–e	5.91 ± 0.335ab	18.45 ± 0.75b	12.80 ± 0.37b	0.323 ± 0.017d	0.0783 ± 0.003c
		750	2.61 ± 0.026bc	6.48 ± 0.085ab	19.58 ± 0.75a	14.06 ± 0.21a	0.411 ± 0.017b	0.0933 ± 0.003a
	250	0	1.11 ± 0.067i	4.24 ± 0.217ab	10.54 ± 0.37gh	8.15 ± 0.21gh	0.071 ± 0.012l	0.0195 ± 0.002l
		250	1.31 ± 0.067hi	4.53 ± 0.300ab	14.18 ± 1.21e	9.03 ± 0.37ef	0.128 ± 0.021k	0.0323 ± 0.004k
		500	1.83 ± 0.015f–h	4.99 ± 0.247ab	16.44 ± 0.57cd	10.54 ± 0.37cd	0.202 ± 0.014i	0.0482 ± 0.003gh
		750	2.50 ± 0.133 b–d	5.24 ± 0.067ab	17.57 ± 0.21bc	12.55 ± 0.21b	0.252 ± 0.032g	0.0590 ± 0.006ef

The same letters within a column indicate there was no significant difference at a 95% probability level at the $p \leq 0.05$ level

HA humic acid; nano-ZnO, zinc oxide nanoparticles, H_2O_2 hydrogen peroxide, $O_2\cdot-$ superoxide radical, *GR* glutathione reductase, *GSH* glutathione reduced, *DHAR* dehydroascorbate reductase, *MDAR* monodehydroascorbate reductase

present study showed that HA priming could improve *GA* expression and decrease *ABA* expression under nano-ZnO stress (Fig. 2b, c, e, f).

The correlation analysis showed that total soluble protein, total soluble sugars, starch content, and electrolyte leakage had a positive significant correlation with seed germination and seedlings growth parameters (Table 3). ABA content and expression level of *OsNCED1* gene had a negative significant correlation with seed germination and seedling characteristics; while *OsABA8ox2* gene expression level showed insignificant correlation (Table 3). Positively significant correlations with GP, SVI, root and shoot length were observed in case of GA_3 content and its related gene (*OsGA20ox2*).

Antioxidant enzymes activities and malondialdehyde content

Mean data regarding APX, CAT, SOD and POD activities and MDA contents were shown in Table 4. The results showed that APX activity was not significantly affected under nano-ZnO stress in both studied cultivars. Seed priming with HA increased APX activity in both cultivars over their respective control (Table 4). In case of CAT and MDA contents, significant increase under all nano-ZnO concentrations was observed (Table 4), except there were no significant increases between 250 and 500 mg L^{-1} nano-ZnO concentrations in CAT activities of unprimed seeds of both cultivars (Table 4). An increasing trend in SOD and POD activities was observed in both cultivars with increasing concentrations of nano-ZnO (Table 4).

ROS accumulation and GR contents

The ROS contents and GR activity linearly increased as nano-ZnO was increased for both cultivars (Table 5). Seed priming with HA had an apparent effect on the H_2O_2 content. Significant increase in H_2O_2 content was observed after exposure to 250 and 500 mg L^{-1} nano-ZnO in both cultivars (Table 5). Similarly, nano-ZnO stress induced gradual enhancement of $O_2\cdot-$ content in both cultivars as compared to the control. The results showed that higher concentration of nano-ZnO (750 mg L^{-1}) induced a significant increase in $O_2\cdot-$ in both rice cultivars (Table 5). Nonetheless, HA priming decreased $O_2\cdot-$ in both cultivars under stress condition. In the present study, the histochemical analysis revealed that higher H_2O_2 concentration indicated by the DAB detection (Fig. 3a) and higher $O_2\cdot-$ content revealed by NBT staining (Fig. 3b) were observed in stressed roots with nano-ZnO as compared with the control. Taken together, the results revealed a significant enhancement in GR and GSH activities in both cultivars under different concentrations of nano-ZnO (Table 5). Moreover, HA priming significantly reduced the activities of GR

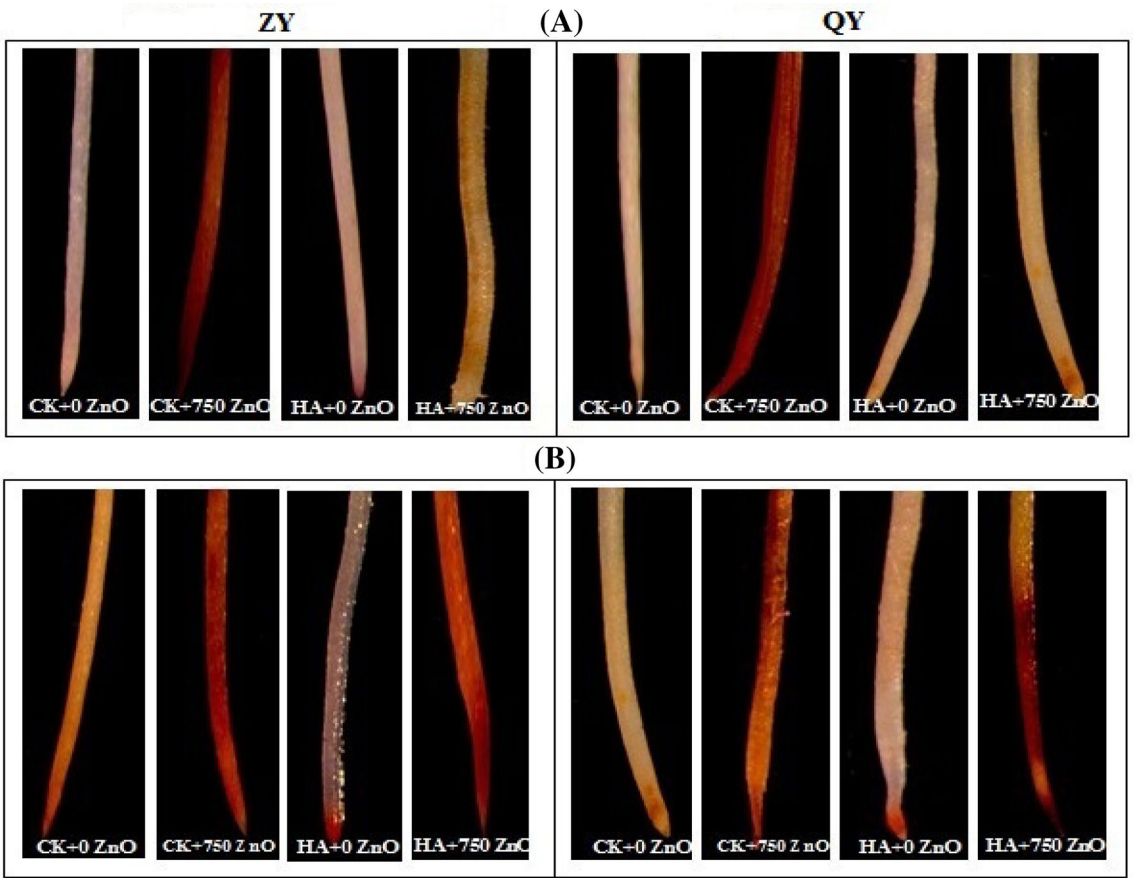

Fig. 3 Effects of nano-ZnO exposure (0 and 750 mg L^{-1}) and priming with HA (250 mg L^{-1}) on reactive oxygen species generation in two cultivars of *Oryza sativa* seedlings. **a** in vivo detection of hydrogen peroxide (H_2O_2) in roots using DAB staining and **b** in vivo detection of superoxide radical ($O_2 \cdot -$) accumulation in roots as revealed by NBT staining. The images were detected using normal light microscope (Leica MZ- g5, Germany)

and GSH in both cultivars under nano-ZnO stress, and the reduction was more obvious in ZY.

DHAR and MDAR activities

Significant increases of DHAR and MDAR activities were observed after exposure to different concentrations of nano-ZnO in both cultivars as compared to their respective controls (Table 5). DHAR activity was somewhat higher in the ZY; while MDAR activity was higher in the QY. Seed priming with HA significantly reduced the activities of DHAR and MDAR of both cultivars under nano-ZnO stress (Table 5).

Ultra-morphology of leaf mesophyll and root tip cells

The transmission electron microscopic (TEM) of the leaf after 14-days of hydroponic exposure plants to nano-ZnO stress (0 and 750 mg L^{-1}) and primed with HA (0 and 250 mg L^{-1}) were shown in Fig. 4. Under the control treatment, clear cell wall (CW), well developed chloroplasts (Ch) with tidy thylakoids (Thy), osmiumphobilic granules (OG) were observed in ZY cultivar (Fig. 4a), while in QY cultivar, a large elongated nucleus (N) with roundish nucleoli (Nue) was observed (Fig. 4e). Plants without nano-ZnO stress, HA priming resulted in clear cell walls (CW), well developed chloroplasts (Ch) in both cultivars (Fig. 4c, g) with tidy granule thylakoids (GT) and osmiumphobilic granules (OG) in ZY (Fig. 4c). The unprimed seeds under nano-ZnO stress showed a degradation of cell morphology with destructed cell wall (CW), a lot of starch grain (SG) (Fig. 4b, f) and vacuoles (Va) was observed in the mesophyll cell of ZY (Fig. 4b). While under stress condition, HA priming improved the leaf mesophyll and cell structure of both cultivars, as little damage in cell wall, few starch grain, developed chloroplast and no vacuole were observed in both cultivars (Fig. 4d, h). The results reported that a high dose of nano-ZnO lead to rupture the structures of all organelles and the size of starch grains was increased.

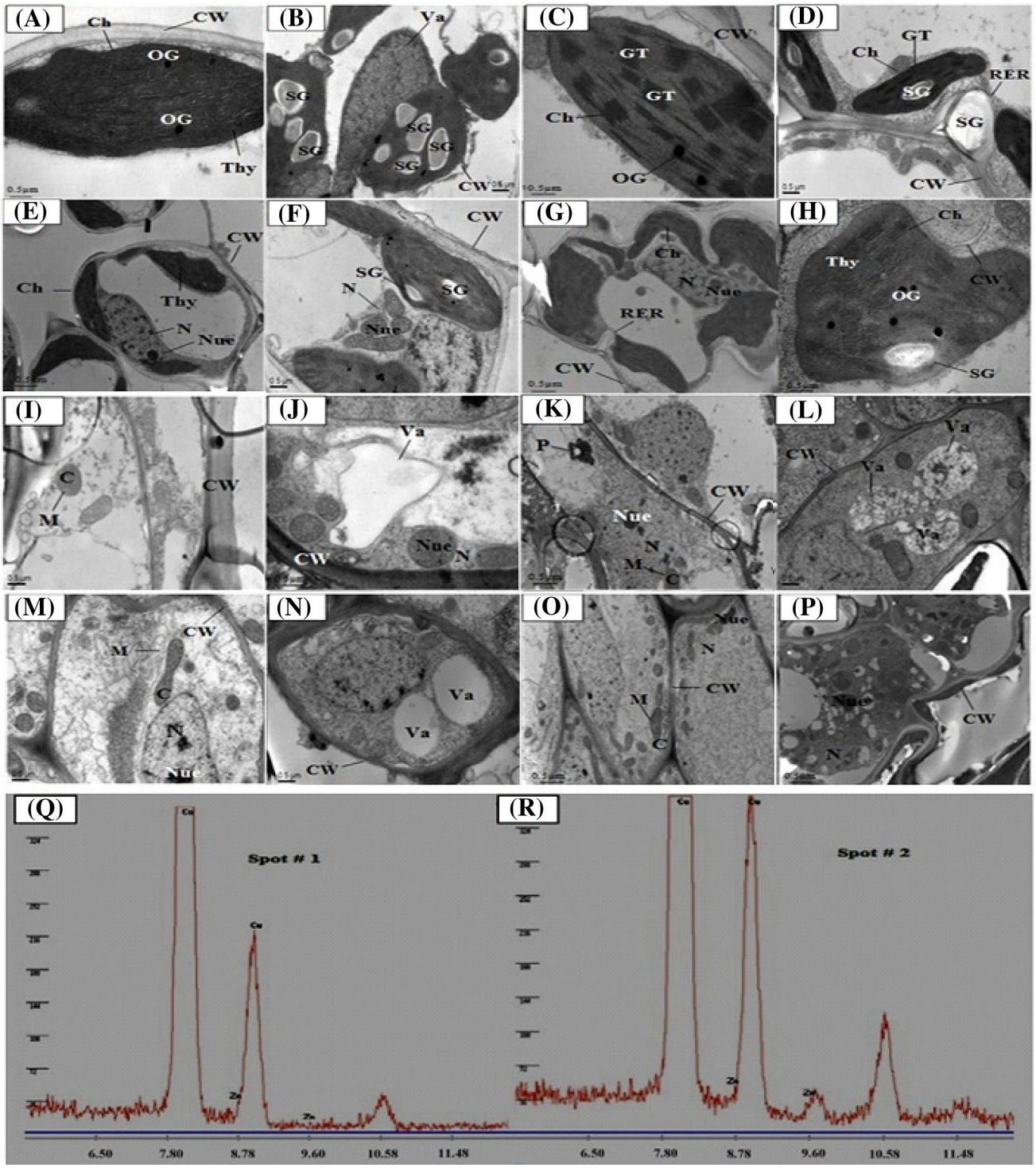

The TEM of root cells for ZY and QY were shown in Fig. 4. TEM analysis of root cells from the control of both cultivars showed a clear and developed cell wall (CW) and oval shaped mitochondria (M) with good cristae in both cultivars (Fig. 4i, m). In addition, well-developed nucleus (N) with roundish nucleoli (Nue) was observed in QY (Fig. 4m). Nano-ZnO at high concentration (750 mg L^{-1}) induced obvious ultrastructural changes in both cultivars over control (Fig. 4j, n). In addition, the nucleus (N) was undeveloped and nuclear membrane was damaged at higher concentration of nano-ZnO (Fig. 4j). Moreover the cell wall was broken and mitochondria could not be observed, indicating a loss of functionality. The TEM analysis of root cells under HA priming under non-stress condition (Fig. 4k, o) showed clear cell wall (CW), a big

◂**Fig. 4** Electron micrographs of leaf mesophyll of 14-days hydroponic exposed seedlings to different concentrations of nano-ZnO (0 and 750 mg L^{-1}) and primed with HA (0 and 250 mg L^{-1}) of two cultivars of *Oryza sativa* (ZY and QY). **a** TEM micrograph of leaf mesophyll cells of ZY under control. **b** TEM micrograph of leaf mesophyll cells of ZY (unprimed with HA and exposed to 750 mg L^{-1} of nano-ZnO). **c** TEM micrograph of leaf mesophyll cells of ZY (primed with HA under control level). **d** TEM micrograph of leaf mesophyll cells of ZY (primed with HA and exposed to 750 mg L^{-1} of nano-ZnO). **e** TEM micrograph of leaf mesophyll cells of QY under control. **f** TEM micrograph of leaf mesophyll cells of QY (unprimed with HA and exposed to 750 mg L^{-1} of nano-ZnO). **g** TEM micrograph of leaf mesophyll cells of QY (primed with HA under control level). **h** TEM micrograph of leaf mesophyll cells of QY (primed with HA and exposed to 750 mg L^{-1} of nano-ZnO). **i** TEM micrograph of root tip cells of ZY under control. **j** TEM micrograph of root tip cells of ZY (unprimed with HA and exposed to 750 mg L^{-1} of nano-ZnO). **k** TEM micrograph of root tip cells of ZY (primed with HA under control level). **l** TEM micrograph of root tip cells of ZY (primed with HA and exposed to 750 mg L^{-1} of nano-ZnO). **m** TEM micrograph of root tip cells of QY under control. **n** TEM micrograph of root tip cells of QY (unprimed with HA and exposed to 750 mg L^{-1} of nano-ZnO). **o** TEM micrograph of root tip cells of QY (primed with HA under control level). **p** TEM micrograph of root tip cells of QY (primed with HA and exposed to 750 mg L^{-1} of nano-ZnO). **q** energy-dispersive spectroscopy (EDS) spectrum of an electron-dense spot of precipitates in root tip cells of ZY cultivar (primed with HA and exposed to 750 mg L^{-1} of nano-ZnO). **r** energy-dispersive spectroscopy (EDS) spectrum of an electron-dense spot of precipitates in root tip cells of ZY cultivar (unprimed with HA and exposed to 750 mg L^{-1} of nano ZnO). Y *bars* reveal the peak counts of the detected heavy metals present in the analyzed spots of electron micrographs

N with Nue and nucleus membrane. In addition, the cell wall and well developed mitochondria could be observed in the micrographs. At high levels of nano-ZnO, the TEM analysis showed unclear cell wall (CW) and undeveloped N with Nue in QY primed seeds (Fig. 4p); while a lot of smaller vacuoles (Va) were observed in the primed ZY seeds than unprimed ones (Fig. 4l). The energy-dispersive spectroscopy (EDS) spectrum of an electron-dense spot confirmed the presence of dense Zn precipitates with a peak at 9.60 nm in the root cells of unprimed seeds of ZY (Fig. 4r, Spot #2), however, did not find a similar peak in the primed seeds (Fig. 4q, Spot #1). Whereas, the other peaks with their relevant organelles showed similar patterns and did not affected by HA priming under nano-ZnO stress (Fig. 4).

Discussion

Seed germination and plant growth

Terrestrial plants can be encountered multitude of nanomaterials in soil through many ways such as potential release from nano-products, sub-surface release for environmental remediation and natural synthesis of nanomaterials (Zhang 2003). The mechanism underlying NPs-impart their toxicity to the biotic receptors such as plant species has not been completely investigated yet (Yin et al. 2012). Our results reported that nano-ZnO decreased the plant growth in terms of seed germination and seedling parameters. In the present study, the decrease in seed germination and seedling growth parameters under nano-ZnO stress was more prominent in QY as compared with ZY. Similar results were earlier reported by Sheteiwy et al. (2016) who reported that QY primed with polyethylene glycol recorded higher germination and seed vigor as compared with ZY under nano-ZnO stress. The differences in germination percentage and seed vigor between both cultivars might be due to the genetically factors and heredity variation in both studied cultivars. Recently, it has been reported that toxicity dose of NPs varies between crops species and the size and concentrations of NPs. In this regards, Lin and Xing (2007) observed that inhibitory concentrations (IC50) caused by nano-ZnO for radish and ryegrass were found to be 50 and 20 mg L^{-1}, respectively. Our study showed that root and shoot length was significantly decreased under nano-ZnO stress. Similarly, it has reported that root elongation in cabbage was not affected by nano-ZnO or nano-$ZnSO_4$ in an excess of 100 µg mL^{-1} exposure level (Pokhrel and Dubey 2013). However, root elongation was totally inhibited and the germination was halted at higher concentrations of nano-$ZnSO_4$. Previous study reported that the decrease in germination percentage might be due to the selective of seed membrane during the seed germination stage might increase the sensitivity to different concentrations of AgNPs during germination (Liu et al. 2010). Present study reported that HA priming improved seed germination percentage and seedlings growth under stress condition. These findings were in harmony with the findings obtained by Sheteiwy et al. (2015) who reported that PEG treatment improved germination and seedling vigor index of *Oryza sativa* under nano-ZnO stress. The inhibition of root elongation under nano-ZnO stress as reported in the present study was in agreement with the findings obtained by Yin et al. (2012) who found out that higher sensitivity of roots to AgNPs might be due to that roots were the first region in direct connection with the medium containing AgNPs.

Soluble sugar is essentially involved in plant stress responses, signal transduction, plant growth, development, storage and so on. In the present study, total soluble sugars, protein and starch contents reduced under nano-ZnO stress, which however improved obviously by HA priming (Fig. 1a–c). It might be due to the detrimental effects of ROS at the cellular level under stress could induce oxidative damage of proteins and consequent denaturation (Martins et al. 2014). Total soluble sugar was a key solute for osmoregulation and protected plants from stress through different mechanisms, including cellular osmotic adjustment, detoxification of ROS, protection of membrane

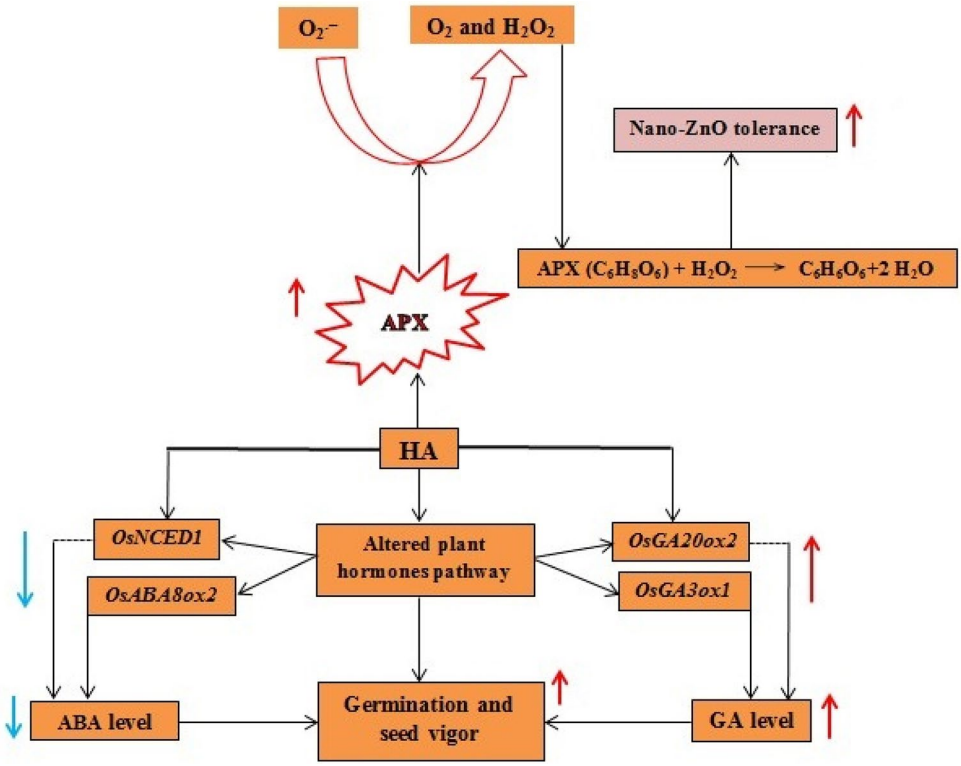

Fig. 5 A comprehensive proposed model shows the underlying mechanism of HA mediating nano-ZnO stress effects in rice seedling. HA positively decreases the activity of ABA through down regulation of *OsNCED1* and *OsABA8ox2* genes expression. On contrast, HA can increase the activity of GA by up regulation of *OsGA3ox1* and *OsGA20ox2* genes expression. Both actions of ABA and GA pathways results in improved germination and seed vigor under nano-ZnO stress. HA can enhance rice tolerance to nano-ZnO stress through increasing APX that can catalyze the partitioning of the superoxide radical ($O_2 \cdot -$) into either ordinary molecular oxygen (O_2) or hydrogen peroxide (H_2O_2). Elevated levels of H_2O_2 can play as a signal molecule to activate stress response pathways and increase rice tolerance to ZnO NPs stress. The *arrow with red* color mean increasing and the *arrow with blue* color mean decreasing. (Color figure online)

integrity and stabilization of proteins and enzymes (Ashraf and Foolad 2007). Therefore, the enhanced electrolyte leakage under nano-ZnO stress (Fig. 1d) might be closely related with the decreased soluble sugar contents.

ABA and GA hormones activities and their relative expression

The relationship between NPs stress and the ABA and GA pathways is rarely investigated during germination stage. Our results suggest that GA catabolism was reduced by excess nano-ZnO stress during germination stage, which results in seed germination inhibition. Conversely, ABA content was increased by nano-ZnO stress as compared to the control (Fig. 2a). In another study, Nambara and MarionPoll (2005) reported that ABA pathway in plants is regulated by ABA catabolism and biosynthesis, both of them are controlled by environmental signals, such as water and temperature. In the present study, genes related with ABA synthesis were significantly up regulated when all nano-ZnO concentrations were applied (Fig. 2b, c), while GA genes showed a reverse trend upon exposed to all nano-ZnO concentrations (Fig. 2e, f). Secondary messengers such as ROS may regulate protein biosynthesis and gene expression associated with the stress defense, however, ROS at higher concentration are reported to be cytotoxic for plants (Jiang and Zhang 2003). In the present study, *OsNCED1* and *OsABA8ox2*, the key genes of ABA catabolism, were decreased and accompanied by the decrease of ABA content in response to HA priming. On the contrary, the relative expression of *OsGA3ox1* and *OsGA20ox2*, the key genes of GA catabolism, were up-regulated and accompanied by the increase of GA levels in response to HA priming. It could be suggested that the feedback regulation of genes induced by HA priming was to meet the metabolic demand for increasing seed germination under stress condition. In addition, the gene expression levels were sometimes not closely correlated with hormone contents, which might be due to the complicated regulation from gene level to metabolism level.

Antioxidant enzymes and ROS accumulation

Under abiotic stress condition, plants can induce antioxidant enzymes, including APX, CAT, SOD and POD to counteract the oxidative stress caused by abiotic stress. Our results showed that plants exposed to nano-ZnO concentrations showed a significant increase in the activities of SOD, POD and CAT as compared to controls plants (Table 4). However, APX activity was decreased upon seed were treated with all nano-ZnO concentrations (Table 4). Recently, Wu et al. (2003) observed an increase in SOD, POD and CAT activities at moderate Cd and a decrease at high concentrations of Cd in barley genotypes stress. Increase of the APX activity in HA-primed seedlings seems to protect stressed seedlings with nano-ZnO through scavenging the H_2O_2 as shown in Fig. 5. However, the lack of complete scavenging of H_2O_2 through enhanced APX activity could be certainly caused higher cell membrane damages in leaves of nano-ZnO stressed rice seedlings. Such findings were also observed by Shaw and Zahed (2013) who reported that enhanced antioxidant enzymes activities of rice seedlings under nano-CuO stress is an indication of an increased production of ROS as well as activation of plants defense mechanism to struggle oxidative stress damage. The increase in SOD activity has been previously reported for different plant species as exposed to toxicity of heavy metals (Qadir et al. 2004). In the present study, CAT activity increased under nano-ZnO stress. CAT activity was reported to be necessary for ROS detoxification under abiotic stress (Gill and Tuteja 2010), and could effectively scavenge H_2O_2 in roots resulted from Pb stress-caused oxidative damage (Reddy et al. 2005). MDA contents were usually used as an indicator of lipid peroxidation as well as oxidative stress damage under abiotic stresses (Chaoui et al. 1997). Our results reported that MDA contents were significantly enhanced in both cultivars upon exposure to different nano-ZnO concentrations (Table 4). Lipid peroxidation could be induced via free radicals such as OH^-, or by lipoxygenase (Panda 2007; Choudhury and Panda 2005). Our results were consistent with those obtained by Halliwell and Gutteridge (1987) who reported that excess ROS reacts with lipids, proteins and nucleic acids leading to increasing of MDA, reduce the membrane stability and DNA damage which cause severe damage to plant cells.

In the present study, ROS were increased in the roots of both *Oryza sativa* cultivars upon exposed to nano-ZnO stress. In this regard, a significant increase in H_2O_2 and MDA levels have been noticed in leaves of rice seedlings exposed to nano-CuO stress (Shaw and Zahed 2013). Priming seed with HA decreased the ROS production in roots under nano-ZnO stress (Table 5). It has reported that nano metal toxicity activated antioxidant enzymes systems which might be beneficial for plants to remove ROS accumulation and inhibit MDA production (Zhang et al. 2010). The GR and GSH activities increased under nano-ZnO stress, while HA priming could significantly reduce their activities in both cultivars (Table 5). This observation was consistent with the findings obtained by Shaw and Zahed (2013) who found that GR and GSH activities in the leaves were significantly increased after exposed to 1 and 1.5 mM of nano-CuO stress in rice seedlings. Interestingly, the nano-copper stressed leaves exhibited decreasing trend in the GR and GSH activity with increasing stress level in barley (Shaw et al. 2014). In the present study, DHAR and MDAR activities were enhanced in nano-ZnO stressed seedlings (Table 5). The increased activities of DHAR and MDAR might be due to the increased GSSG content induced by nano-ZnO stress. However, it was inconsistent with the findings obtained by Shaw et al. (2014) who found that the DHAR and MDAR activities reduced in nano-copper stressed leaves of 20-day barley.

Ultrastructure observation

The ultrastructure study is necessary in plant cells under nano-ZnO stress due to the uptake of nano-ZnO doses in rice seedling tissues. It has stated that transmission microscopy helped to detect the damage at the cellular level, providing the basis and insights for potential impact of transmission electron macroscopic study under abiotic stress (Shaw et al. 2014). In the current study, the mesophyll and root cells of *Oryza sativa* showed significant changes under nano-ZnO stress conditions. Under higher concentrations of nano-ZnO, ruptured cell wall and several vacuoles as well as increase in starch grain size were observed in both cultivars. In this regard, increased starch grain size under heavy-metal stress indicates that plants might be undergoing stress (Daud et al. 2009). In the present study, the root and leaf cell ultrastructure were improved by HA priming under nano-ZnO stress, and the enhancements were more obvious in QY as compared with ZY. It might be due to the better nano-ZnO tolerance of QY than ZY. These results were consistent with our previous study (Sheteiwy et al. 2015) which reported that priming with polyethylene glycol improved the cell ultrastructure of QY and ZY under nano-ZnO stress with more prominent in QY. In addition, earlier studies reported heavy metal badly disrupts the thylakoid membranes in *Brassica. napus* plants, damaged the root ultrastructure, diluted of nucleolus and breakage of nuclear membrane (Qian et al. 2014), increasing the metal uptake in plants (Gill et al. 2014). Therefore, the improvement of HA on cell ultrastructure suggested that HA might contribute to the membrane repairation under nano-ZnO stress.

Conclusions

Priming with HA improved the physiological parameters in terms of seed germination, seedling growth, the content of protein, sugars and starch under nano-ZnO stress. The stress effect of nano-ZnO increased ABA and decreased GA contents in rice seeds. Further, the increases of antioxidant enzymes and accumulation of ROS under stress indicated the activation of plants defense mechanisms to reduce oxidative stress damage. HA regulates ABA and GA hormones signaling, which could improve the germination percentage and rice seed vigor under stress condition. In addition, HA also improved the APX activity pathway which help to degrade both $O_2 \cdot -$ and H_2O_2 and thereby increased the tolerance of rice under nano-ZnO stress. The excess ROS generation might result in the death of root tip as a result of nano-ZnO stress. The ultra-morphology analysis revealed that HA priming improved cell ultrastructure of the root tip and leaf mesophyll under nano-ZnO stress. The current research has provided potential insights regarding the effect of HA priming on the rice germination and seedling growth under nano-ZnO stress. However, future perspective research is needed for exploring the concentration of nanoparticles in the soil profile as nanomaterials application has increased in the recent years leading to significant increase of their traces in the environment.

Acknowledgements This research was supported by the National Natural Science Fund (Nos. 31201279, 31371708, 31671774), Zhejiang Provincial Natural Science Foundation (LZ14C130002, LY15C130002), the Project of the Science and Technology Department of Zhejiang Province (Nos. 2013C02005), Dabeinong Funds for Discipline Development and Talent Training in Zhejiang University and Jiangsu Collaborative Innovation Center for Modern Crop Production, P.R. China.

References

Ashraf M, Foolad MR (2007) Roles of glycine betaine and proline in improving plant abiotic stress resistance. Environ Exp Bot 59:206–216

Asli S, Neumann PM (2010) Rhizosphere humic acid interacts with root cell walls to reduce hydraulic conductivity and plant development. Plant Soil 336:313–322

Blaylock MJ, Huang JW (2000) Phytoextraction of metals. In: Raskin I, Ensley BD (eds) Phytoremediation of toxic metals: using plants to clean up the environment. Wiley, Toronto, p 303

Bradford NM (1976) Rapid and sensitive method for quantitation of microgram quantities of protein utilizing principle of protein-dye binding. Anal Biochem 72:248–254

Chaoui A, Mazhoudi S, Ghorbal MH, Ferlani EE (1997) Cadmium and zinc induction of lipid peroxidation and effects on antioxidant enzyme activities in bean (*Phaseolus vulgaris* L.). Plant Sci 127: 139–147

Choudhury S, Panda SK (2005) Toxic effect, oxidative stress and ultrastructural changes in moss *Taxitheelium nepalense* (Schwaegr.) Broth. under lead and chromium toxicity. Water Air Soil Pollut 167:73–90

Daud MK, Variath MT, Ali S, Najeeb U, Muhammad J, Hayat Y, Dawood M, Khan MI, Zaffar M, Sardar AC, Tong XH, Zhu S (2009) Cadmium-induced ultramorphological and physiological changes in leaves of two transgenic cotton cultivars and their wild relative. J Hazard Mater 168:614–625

Daud MK, Quiling H, Lei M, Ali B, Zhu SJ (2015) Ultrastructural, metabolic and proteomic changes in leaves of upland cotton in response to cadmium stress. Chemosphere 120:309–320

Finch-Savage WE, Leubner-Metzger G (2006) Seed dormancy and the control of germination. New Phytol 171:501–523

Gill SS, Tuteja N (2010) Reactive oxygen species and antioxidant machinery in abiotic stress tolerance in crop plants. Plant Physiol Biochem 48:909–930

Gill RA, Hu XQ, Ali B, Yang C, Shou JY, Wu YY, Zhou WJ (2014) Genotypic variation of the responses to chromium toxicity in four oilseed rape cultivars. Biol Plant 58:539–550

Halliwell B, Gutteridge JMC, Aruoma O (1987) The deoxyribose method: a simple 'test tube' assay for determination of rate constants for reactions of hydroxyl radicals. Anal Biochem 165:215–219

Hu Q, Fu Y, Guan, Y, Lin C, Cao D, Hu W, Sheteiwy M, Hu J (2016) Inhibitory effect of chemical combinations on seed germination and pre-harvest sprouting in hybrid rice. Plant Growth Regul 80:281–289

International Seed Testing Association (ISTA) (2004) Seed Sci Technol 24: 1–335

Jiang M, Zhang J (2003) Effect of abscisic acid on active oxygen species, antioxidative defence system and oxidative damage in leaves of maize seedlings. Plant Cell Physiol 42:1265–1273

Kool PL, Ortiz MD, Gastel VCA (2011) Chronic toxicity of ZnO nanoparticles, non-nano ZnO and $ZnCl_2$ to *Folsomia candida* (Collembola) in relation to bioavailability in soil. Environ Pollut 159:2713–2719

Law MY, Charles SA, Halliwell B (1983) Glutathione and ascorbic-acid in spinach (*Spinacia oleracea*) chloroplasts, the effect of hydrogen-peroxide and of paraquat. Biochem J 210:899–903

Lesmana SO, Febriana N, Soetaredjo FE, Sunarso J, Ismadji S (2009) Studies on potential applications of biomass for the separation of heavy metals from water and waste water. Biochem Eng J 44:19–41

Lin D, Xing B (2007) Phytotoxicity of nanoparticles: inhibition of seed germination and root growth. Environ Pollut 150:243–250

Liu Y, Ye N, Liu R, Chen M, Zhang J (2010) H_2O_2 mediates the regulation of ABA catabolism and GA biosynthesis in *Arabidopsis* seed dormancy and germination. J Exp Bot 61:2979–2990

Mahmoud A, Ezgi O, Merve A, Ozhan G (2016) In vitro toxicological assessment of magnesium oxide nanoparticle exposure in several mammalian cell types. Int J Toxicol 35:429–437

Martins LL, Mourato MP, Baptista S, Reis R, Carvalheiro F, Almeida AM, Fevereiro P, Cuypers A (2014) Response to oxidative stress induced by cadmium and copper in tobacco plants (*Nicotiana tabacum*) engineered with the trehalose-6-phosphate synthase gene (*AtTPS1*). Acta Physiol Plant 3:755–765

Meloni A, Oliva MA, Martinez CA, Cambraia J (2003) Photosynthesis and activity of superoxide dismutase, peroxidase and glutathione reductase in cotton under salt stress. Environ Exp Bot 49:69–76

Miyake C, Asada K (1992) Thylakoid-bound ascorbate peroxidase in spinach chloroplasts and photoreduction of its primary oxidation product monodehydroascorbate radicals in thylakoids. Plant Cell Physiol 33:541–553

Moghadam HRT (2013) Humic acid as an ecological pathway to protect corn plants against oxidative stress. Biological Forum 7:1704–1709.

Nakano Y, Asada K (1981) Hydrogen peroxide is scavenged by ascorbate specific peroxidase in spinach chloroplast. Plant Cell Physiol 22:867–880

Nambara E, Marion-Poll A (2005) Abscisic acid biosynthesis and catabolism. Plant Biol 56:165–185

Panda SK (2007) Chromium-mediated oxidative stress and ultrastructural changes in root cells of developing rice seedlings. J Plant Physiol 164:1419–1428

Parera CA, Cantliffe DJ (1994) Pre-sowing seed priming. Hortic Rev 16:109–141

Pokhrel LR, Dubey B (2013) Evaluation of developmental responses of two crop plants exposed to silver and zinc oxide nanoparticles. Sci Total Environ 453:321–332

Qadir S, Qureshi MI, Javed S, Abdin MZ (2004) Genotypic variation in phytoremediation potential of *Brassica juncea* cultivars exposed to Cd stress. Plant Sci 167:1171–1181

Qian P, Sun R, Ali B, Gill RA, Xu L, Zhou WJ (2014) Effects of hydrogen sulfide on growth, antioxidative capacity, and ultrastructural changes in oilseed rape seedlings under aluminum toxicity. J Plant Growth Regul 33:526–538

Reddy AM, Kumar SG, Jyothsnakumari J, Thimmanaik S, Sudhakar C (2005) Lead induced changes in antioxidant metabolism of horsegram (*Macrotyloma uniflorum* (Lam.) Verdc.) and bengalgram (*Cicer arietinum* L.). Chemosphere 60:97–104

Schaedle M, Bassham JA (1977) Chloroplast glutathione reductase. Plant Physiol 59:1011–1012

Shaw AK, Zahed H (2013) Impact of nano-CuO stress on rice (*Oryza sativa* L.) seedlings. Chemosphere 93:906–915

Shaw AK, Supriya G, Hazem MK, Karolina B, Marian B, Marek Z, Zahed H (2014) Nano-CuO stress induced modulation of antioxidative defense and photosynthetic performance of Syrian barley (*Hordeum vulgare* L.). Environ Exp Bot 102:37–47

Sheteiwy MS, Guan Y, Cao D, Li J, Nawaz A, Hu Q, Hu W, Ning M, Hu J (2015) Seed priming with polyethylene glycol regulating the physiological and molecular mechanism in rice (*Oryza sativa* L.) under nano-ZnO stress. Sci Rep 5:14278

Sheteiwy MS, Fu Y, Hu Q, Nawaz A, Guan Y, Li Z, Huang Y, Hu J (2016) Seed priming with polyethylene glycol induces antioxidative defense and metabolic regulation of rice under nano-ZnO stress. Environ Sci Pollut Res 23:19989–20002

Sheteiwy M, Shen H, Xu J, Guan Y, Song W, Hu J (2017) Seed polyamines metabolism induced by seed priming with spermidine and 5-aminolevulinic acid for chilling tolerance improvement in rice (*Oryza sativa* L.) seedlings. Environ Exp Bot 137:58–72

Valipour M (2013a) Evolution of irrigation-equipped areas as share of cultivated areas. Irrig Drain Sys Eng 2:1

Valipour M (2013b) Use of surface water supply index to assessing of water resources management in Colorado and Oregon. US 3:631–640

Valipour M (2015) Land use policy and agricultural water management of the previous half of century in Africa. Appl Water Sci 5:367–395

Velikova V, Yordanov I, Edreva A (2000) Oxidative stress and some antioxidant systems in acid rain-treated bean plants. Plant Sci 151:59–66

Viero DP, Valipour M (2017) Modeling anisotropy in free-surface overland and shallow inundation flows. Adv Water Res 104:1–14

Wu F, Zhang G, Dominy P (2003) Four barley genotypes respond differently to cadmium: lipid peroxidation and activities of antioxidant capacity. Environ Exp Bot 50:67–78

Yin L, Colman BP, McGill BM, Wright JP, Bernhardt ES (2012) Effects of silver nanoparticle exposure on germination and early growth of eleven wetland plants. PLoS ONE 7:1–7

Zhang W (2003) Nanoscale iron particles for environmental remediation: an overview. J Nanopart Res 5:323–332

Zhang H, Hu LY, Li P, Hu KD, Jiang CX, Luo JP (2010) Hydrogen sulfide alleviated chromium toxicity in wheat. Biol Plant 54:743–747

Zhou WJ, Leul M (1999) Uniconazole-induced tolerance of rape plants to heat stress in relation to changes in hormonal levels, enzyme activities and lipid peroxidation. Plant Growth Regul 27:99–104

Zhu JK (2000) Genetic analysis of plant salt tolerance using *Arabidopsis*. Plant Physiol 124:941–948

Zhu G, Ye N, Zhang J (2009) Glucose-induced delay of seed germination in rice is mediated by the suppression of ABA catabolism rather than an enhancement of ABA biosynthesis. Plant Cell Physiol 50:644–651

Zhu L, Cao D, Hu Q, Guan Y, Hu W, Nawaz A, Hu J (2015) Physiological changes and *sHSPs* genes relative transcription in relation to the acquisition of seed germination during maturation of hybrid rice seed. J Sci Food Agric 96:1–8